Biomimetic tissue-engineered anterior cruciate ligament replacement

James A. Cooper, Jr.*†, Janmeet S. Sahota†, W. Jay Gorum II†, Janell Carter†, Stephen B. Doty‡, and Cato T. Laurencin*†§¶‖**

*School of Biomedical, Engineering, Science, and Health Systems and †Center for Advanced Biomaterials and Tissue Engineering, 3141 Chestnut Street, Drexel University, Philadelphia, PA 19104; ‡Hospital for Special Surgery, 535 East 70th Street, New York, NY 10021; §Department of Orthopaedic Surgery, University of Virginia Health System, P.O. Box 800159, Charlottesville, VA 22903; and Departments of ¶Biomedical Engineering and ‖Chemical Engineering, University of Virginia, Charlottesville, VA 22903

There are >200,000 anterior cruciate ligament (ACL) ruptures each year in the United States, and, due to the poor healing properties of the ACL, surgical reconstruction with autograft or allograft tissue is the current treatment of these injuries. To regenerate the ACL, the ideal matrix should be biodegradable, porous, and exhibit sufficient mechanical strength to allow formation of neoligament tissue. Researchers have developed ACL scaffolds with collagen fibers, silk, biodegradable polymers, and composites with limited success. Our group has developed a biomimetic ligament replacement by using 3D braiding technology. In this preliminary in vivo rabbit model study for ACL reconstruction, the histological and mechanical evaluation demonstrated excellent healing and regeneration with our cell-seeded, tissue-engineered ligament replacement.

biomaterials | regenerative medicine

This study was conducted to evaluate the performance of a polymeric 3D braided fibrous tissue-engineered anterior cruciate ligament (ACL) replacement for use in ACL reconstruction. The feasibility of this approach was investigated by comparison of cell-seeded and unseeded tissue-engineered ligaments (TELs) with a rabbit model. The key concepts investigated were (*i*) the in vivo response of allograft cells seeded onto TELs, (*ii*) the effect of porosity and pore interconnectivity on cell and collagen infiltration, (*iii*) the capability of the implant to allow for vascularization, and (*iv*) the capability of the implant to maintain mechanical function and to transfer load to the neoligament.

Several groups have explored ligament-like scaffolds with collagen fibers, silk, biodegradable polymers and composites with limited success (1–6). During this study, we fabricated an absorbable polyL-lactide (PLLA) 3D, braided TEL replacement capable of supporting the growth and phenotypic expression of cells when seeded in vitro. There have been several published observations of favorable PLLA device interactions in animal and human clinical studies (2, 4, 7–10). The degradation of PLLA from a chemical standpoint in vivo can be categorized into five stages (2, 7). These stages are hydration, depolymerization, loss of mass integrity, absorption, and elimination. This polymer was chosen because of its mechanical retention and its in vitro cellular response to primary rabbit ACL cells (6, 11–14).

Rabbits are one of the most commonly used animals for orthopedic surgery in vivo studies (1, 15–24). Adult New Zealand White rabbits were used in this study because rabbits are relatively high-level vertebrates, having a size that enables surgical operations, convenient histology, and mechanical analysis. In addition, there was data on ACL reconstruction in rabbits with bone–patellar tendon–bone autografts (the gold standard for human reconstructions) that could be used to compare with our tissue engineered ligament results (20).

The goal of this investigation was to develop and study a tissue-engineered ACL replacement that could eventually be used for humans. This study was conducted to determine the effectiveness of our TEL replacement in a rabbit before moving to a larger animal.

Results

The ligament replacements were designed to be slightly smaller than the original rabbit ACL controls to allow for tissue ingrowth. This scaffold design was advantageous because a fibrous capsule initially surrounds the ligament replacements at 4 weeks, followed by infiltration across the replacement by collagen tissue. The histological section of normal rabbit ACL tissue shows the crimp nature of the collagen fibers and the sparse cellular population of the ligament tissue (Fig. 1*A*).

The collagen infiltration into the 4-week unseeded TEL replacement occurred at the periphery of the replacement, and the collagen synthesized within that time period was not strongly attached, which resulted in the polymer filaments falling out of the section during processing. In addition, the sections of the 4-week unseeded implant that remained intact showed hypercellularity with the presence of fibroblast, mononuclear, and giant cells (data not shown).

The 4-week seeded TEL sections showed the presence of a fibrous capsule and tissue infiltration at the periphery of the implant. The tissue ingrowth into the seeded TEL was better than the unseeded TEL, which prevented fewer polymer filaments from falling out during processing. The sections showed that collagen and cellular infiltration was concentrated at the periphery of the implant because of the spacing between the filaments. At the edge of the scaffold, the cells are able to maneuver around the polymer filaments and produce collagen tissue, whereas in the central region of the implant, the cell migration is slowed because of the spacing between filaments.

The collagen and cellular infiltration into the 12-week unseeded TEL was throughout the replacement. The collagen synthesized within this time period was strongly attached, which resulted in the polymer filaments not falling out of the section during processing (Fig. 1*B*). In addition, the section of the 12-week unseeded implant showed segmentation, vascularization, collagen tissue ingrowth, and a decrease of the fibrous capsule. The connective tissue synthesized throughout the implant was not dense or oriented (Fig. 1 *C* and *D*) and remained hypercellular with the presence of fibroblast, mononuclear, and
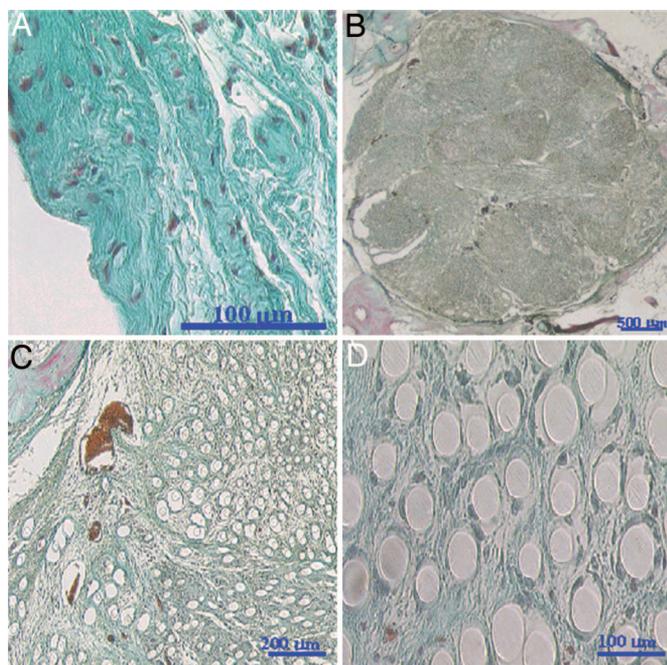
APPLIED BIOLOGICAL SCIENCES

Fig. 1. Histology of native ACL and TEL. (*A*) Rabbit ACL control histological section. (*B*) Cross-section of entire 12-week unseeded TEL replacement showing thin fibrous capsule, vascularization, and collagen tissue ingrowth. (*C*) Blood vessel near the edge of the implant. (*D*) Nonoriented collagen tissue formation at the center of the implant. Weigert's Trichrome stain was used throughout. Red–purple indicates fibroblasts and blood vessels, and blue–green indicates collagen.

Fig. 2. Sections of 12-week seeded TEL replacement. (*A*) Cross-section of entire replacement. (*B*) Cells and collagen tissue encircling the polymer filaments. (*C*) Cells producing collagen fibrils near the edge of the implant. (*D*) Sparse cell population and mature collagen ingrowth near the center of the implant. Safranin O stain was used throughout. Red–purple indicates fibroblasts, blue–green indicates collagen, and white circles indicate polymer filaments.

giant cells. Some of the multinucleated giant cells were seen on the periphery of the scaffold trying to engulf the polymer filaments. Also the polymer filaments showed no signs of fragmentation and remained relatively intact. The sections also revealed blood vessels within the implant with dense collagen fibers encapsulating the vessels and the erythrocytes (Fig. 1*C*).

The 12-week seeded TEL sections showed the presence of a dense connective tissue that was infiltrated throughout the replacement (Fig. 2*A*). Sections of the 12-week unseeded TEL replacement also showed segmentation and vascularization. The tissue ingrowth into the seeded TEL was greater than the unseeded TEL, and the fibrous capsule was less apparent (Fig. 2*A*). In addition, the collagen produced was in a fibrous form surrounding the polymer filaments (Fig. 2*B*). At the edge of the scaffold, the cells are able to maneuver around the polymer filaments and were producing collagen fibers, whereas in the central region of the implant, there were fewer cells that moved freely through the spacing between filaments surrounded by dense collagen tissue that gives an indication of the connective tissue and cellularity after tissue remodeling (Fig. 2 *C* and *D*).

The results of tensile testing of the native rabbit ACL controls, TEL, and seeded TEL were recorded for each time point at 4 and 12 weeks. The values and uncertainty were represented by means and standard deviations. The ligament replacements were in direct contact with bone so that the ingrowth was the primary mode of fixation, and this *in vivo* study helped to determine the strength as a function of implantation time (Table 1). The cross-sectional areas of the rabbit ACL and ligament replacements were measured under slight tension. The unseeded and seeded TELs after pull-out from both of the bone tunnels were placed into the grips and tested to failure (Fig. 3). The polymer–tissue implants failed during testing in the intraarticular zone. The tensile data showed that the TEL and seeded TEL load-carrying capacity decreased over the implantation period.
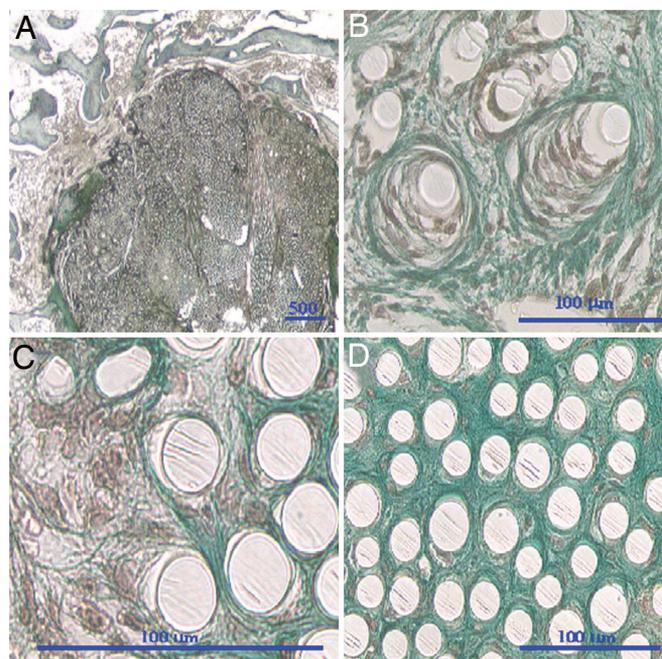
12-week time point, five of six unseeded TELs and three of six seeded TELs ruptured. The percent of strength retention of the TEL as a percentage of native rabbit ACL control maximum load was $67 \pm 23\%$ at 4 weeks ($n = 6$) and decreased to 11% by the 12-week time point ($n = 1$). In addition, the percent of strength retention of the cell-seeded TEL as a percentage of rabbit ACL control maximum load was $76 \pm 14\%$ at 4 weeks ($n = 6$) and decreased to $30 \pm 6\%$ by the 12-week time point ($n = 3$), which was an improvement over the TELs without cells. There was no significant difference in mechanical properties between the unseeded and seeded TEL at the 4-week time point. In addition, at that time point, the loads of the knee were being totally handled by the replacements. The tensile mechanical properties of the native rabbit ACL controls and TEL replacements were compared with other studies (Table 2).

The typical load-deformation and stress–strain curves of the 3D 5×5 PLLA square braided scaffold (TEL) used as a control of the polymer scaffold without implantation was tested at a strain rate of 2% per second to failure ($n = 6$) (Fig. 3*A*). Also, the load-deformation and stress–strain curves of the native rabbit ACL controls were tested at a strain rate of 2% per second to failure ($n = 6$) (Fig. 3*D*). The rabbit ACL curves demonstrated the typical behavior of the ligament, which comprised a toe region (ligament not under stress), linear region (recruitment of collagen fibers under stress), microfailure region (instability in curve just before failure), and failure region (rupture of ligament midsubstance) (25–33). The behavior of the ligament corresponds to the straightening of the crimped collagen fibers in which increasing amounts of load caused displacement of the tissue. The 12-week sample curves are more linear than 4-week curves and more comparable to the ACL control curves shown in Fig. 3*D*. The 12-week curves also seem to have more of a toe region (Fig. 3 *E* and *F*). The nonlinear force-deformation behavior of ligaments occurs because of flattening of the crimp

Table 1. Mechanical properties of native rabbit ACL, unseeded TEL, and seeded TEL replacements

Sample (no.)	Maximum load, N	Young's modulus, MPa	Extension at maximum load, mm
Native rabbit ACL control (20)	314.3 ± 68	181.2 ± 132.2	3.9 ± 1.8
5 × 5 3D square braid TEL (6)	332.2 ± 19.6	354.4 ± 68.5	4.7 ± 0.24
Four-week unseeded TEL (6)	209.0 ± 73.5	103.0 ± 53.9	3.5 ± 0.59
Four-week seeded TEL (6)	239.0 ± 43	108.4 ± 27.7	4.1 ± 1.2
Twelve-week unseeded TEL (1)	35	3.0	11.4
Twelve-week seeded TEL (3)	92.8 ± 18.4	53.8 ± 15.1	3.9 ± 2.0

of collagen fibers and heterogeneous distribution of collagen fibers. As force increases, the ligament becomes stiffer to provide resistance to increasing deformations and to protect the joint. The toe region of the load-deformation curve is thought to correspond with the stretching out of the crimp. For the polymeric braided scaffolds, there is little crimp or gradual recruitment of fibers; all of the fibers in the braid are recruited at the same time. The total recruitment of fibers of the whole scaffold under tension is shown in the linear region on the graphs (linear stiffness). The net stiffness of the natural ligament structure begins to fail as the linear region decays, which is due to the collagen fibers failing with increasing force, leading to gross structural failure through all of the collagen fibers. However, with the 3D, braided TEL, there is some resistance to the total failure of the structure due to the nature of 3D braiding technology, which resists total failure of the structure and

gradually fails until there are too few fibers to resist the load. These are the mechanical behaviors shown in Fig. 3.

Discussion

To properly test the efficacy of the 3D PLLA 5 × 5 square braid TEL replacement for ACL reconstruction, a rabbit model was chosen, because the size and anatomic dimensions of the rabbit knee are approximately one-fourth the size of the human ACL. The ACL limits the joint motions of the knee and may be more important in the quadruped rabbits than in the biped humans (34).

A simple subcutaneous placement to test for tissue compatibility would not be useful for this study even though past researchers have tried this technique for biodegradable and nondegradable materials (4, 15). The objective of this study was to investigate the ingrowth of new ligament tissue into the scaffolds that are seeded with ACL cells. In addition, the synovial environment of the knee is different from the subcutaneous environments due to its low vascularity. Evaluation with histology was performed to observe any inflammatory response and to evaluate the vasculature distribution within the replacement. Vasculature within the implant would allow for tissue infiltration and acts as a conduit for mesenchymal stem cells to enter the scaffolds. In addition, the biomechanical response of the ligament replacement to maintain normal knee function without failure has been tested, and postmortem mechanical testing was performed on the ligament replacements to determine strength retention of the implant over time.

The observation of the rabbits after surgery showed that the rabbits were weight-bearing within 24 h of surgery. Within the first week, the animals ate very little, which could have been caused by the administration of the antibiotics and drugs for pain. After a week, the animals regained their appetites after the removal of the staples and began to gain weight. Most of the swelling that occurred in the left legs (location of surgery) was concentrated around the medial and lateral locations of the suture buttons. This swelling was also observed grossly when the buttons were removed from the legs in preparation for mechanical testing. The 12-week replacements that ruptured before mechanical testing always ruptured in the intraarticular zone (midsubstance) and had a mop like bushy end appearance at the insertion sites.

The histological sections of the intraarticular zone showed excellent tissue infiltration through the implants near the end of the implantation period. The original control sections of the rabbit ACL normal tissue showed a sparse population of fibroblast-like cells and crimped collagen fibers. A fibrous capsule at the 4-week time point and fiber separation due to new tissue ingrowth caused an enlargement of the cross-sectional area of the replacement in the intraarticular zone. At the 4-week time point, there was a weak penetration of collagen tissue ingrowth into the periphery of the ligament replacement at the surface. At 4 weeks, cells produced collagen matrix but showed no tissue infiltration to the center of the scaffold due to the lack of spacing
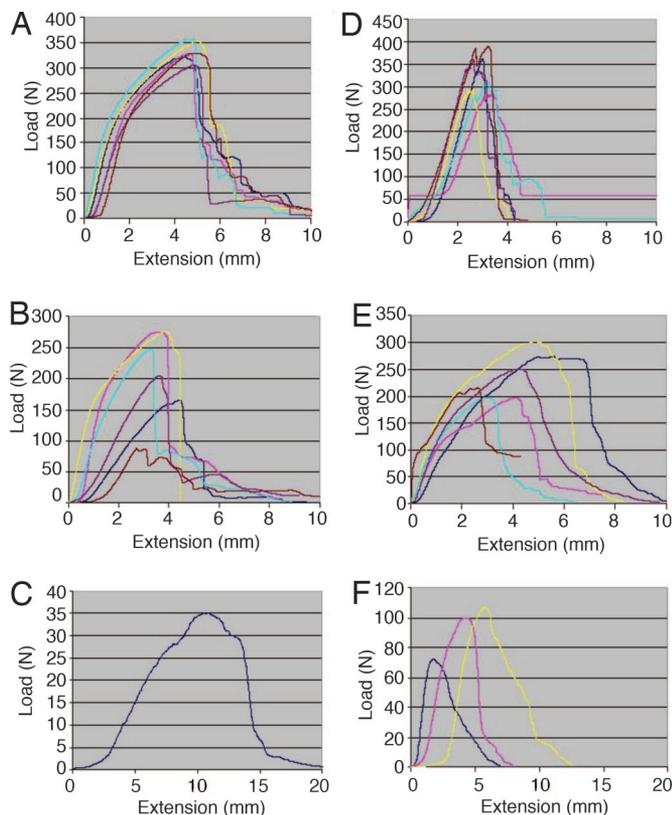

Fig. 3. Load-deformation graphs measured at 2% per second. (*A*) Control 5 × 5 PLLA 3D square braids before implantation (unseeded TEL replacement) (*B*) Four-week unseeded TEL. (*C*) Twelve-week unseeded TEL. (*D*) Native rabbit ACL (contralateral legs). (*E*) Four-week seeded TEL. (*F*) Twelve-week seeded TEL.

Table 2. Maximum tensile load data comparing the unseeded and seeded TEL replacements with other *in vivo* studies that performed ACL reconstructions

| Animal model | Implant | Animal native ACL, N | Maximum tensile loads, N | | | | | Refs. |
			4 wk	6 wk	12 wk	20 wk	30 wk	
Rabbit	Unseeded TEL	314 ± 68	209 ± 74	—	35	—	—	—
Rabbit	Seeded TEL	314 ± 68	239 ± 43	—	93 ± 18	—	—	—
Rabbit	Collagen	251 ± 47	10	—	—	32	—	(1)
Rabbit	Autograft patellar tendon	418	—	26 ± 5	—	—	63 ± 19	(20)
Sheep	PLLA ligament augmentation device	848 ± 529	—	79 ± 51	124 ± 90	—	—	(34)

Maximum tensile loads are shown at 4, 6, 12, 20, and 30 weeks after implementation.

between the filaments. This phenomenon has been observed in other studies in which collagen infiltration into the replacement was limited to the periphery due to a lack of pore interconnectivity (5). The fibrous capsule observed at the 4-week time point decreased in size by the end of the study period at the 12-week time point. At 12 weeks, the scaffolds showed a decreased fibrous capsule, penetration of tissue to the center of the scaffold, and areas of remodeled collagen tissue with sparse cellular population, as seen in the native rabbit ACL control sections. The polymer filaments showed no visible decrease in size and no signs of fragmentation during the implantation period; signs of cracking were due to processing artifacts. The replacements showed high cellularity and very active fibroblast cells as compared with the native rabbit ACL, which would be normal for any implanted device. A mild inflammatory response to the PLLA scaffold during the implantation period was observed as indicated by the presence of foreign body reaction and giant cells within the intraarticular zone of the TELs. Revascularization of the ligament replacement was shown at the 12-week time point by the appearance of blood vessels. In addition, the 12-week time points of both replacements showed infiltration of collagen tissue between filaments and yarns throughout the implant. The differences between the unseeded TELs and seeded TELs were the amount and quality of the collagen synthesized and the rate of tissue remodeling. The infiltration and accumulation of collagen in the unseeded TEL was not oriented or aligned, whereas the infiltration of collagen tissue within the seeded TEL showed oriented collagen fibers capable of withstanding mechanical load transfer. The denseness and infiltration of the collagen tissue between the yarns and filaments of the seeded TEL is comparable with observations made with other ligament replacements 11–48 months after implantation (5). In addition, Guidoin *et al.* (5) concluded from their studies that there was no correlation between the duration of implantation and the degree of collagen infiltration, which means that our designed scaffold had the proper pore size and interconnectivity to promote collagen development, maturation, and orientation within and around the replacement.

The mechanical properties of the ligament replacements are affected not only by the mechanical strength of the PLLA 3D scaffold but also by fixation to the bone, graft positioning in the tunnels, biomechanical stress factors due to dynamic loading, and the rate of tissue ingrowth in the intraarticular zone and bone tunnels. The early postoperative period is critical to the healing process of the reconstructed ACL, as was apparent in the histological sections showing a lack of tissue ingrowth during the first 4 weeks. In addition, the collagen tissue-remodeling period that is critical to the success of the implant occurs by the 12th week. The 12-week unseeded TEL observed by histology showed infiltration to the center of the implant, but the tissue did not have enough time to handle the transfer of mechanical load. The initial tensile loads were maintained during the first 4 weeks for both the unseeded and seeded TEL. The 3D, braided

ligament was designed to gradually transfer the load of the intraarticular joint to the cells and for collagen infiltrating the TEL to eliminate stress-shielding. Initially, the tensile loads are provided for by the braided structure, as observed at the 4-week time point. But as healing occurs and the braided structure becomes weaker, the tensile loads are supported by the neoligament tissue and the braid. At 12 weeks, there was a difference between the capacity of the unseeded and seeded TEL to handle the load transfer to the neoligament. The unseeded TEL had five of six replacements rupture, whereas the seeded TEL had three of six replacements rupture in the intraarticular zone. This inability to maintain the load is most likely due to the fatigue of the PLLA fibrous scaffold in combination with the slow rate of collagen tissue synthesis and remodeling. The seeded TELs retained more of their tensile strength compared with the unseeded TELs due to the preseeded cells that resulted in more connective tissue and that oriented collagen fibers. The strength retention of the maximum tensile loads at the 12-week time point compared with the native rabbit ACL controls were 11% and 30% for the unseeded and seeded TEL, respectively. The strength retention of the 12-week seeded TEL was much greater when compared with the autograft (gold standard) study by Ballock *et al.* (20) at 30 weeks, which showed a strength retention in rabbits of 15%; when compared with the collagen prosthesis of Dunn *et al.* (1) at 20 weeks, which showed a strength retention in rabbits of 13%; and when compared with the research of Laitinen *et al.* (34) on sheep with a PLLA implant as a ligament augmentation device, which showed strength retention of 15% of the maximum load of the control ACL at 12 weeks. The TEL replacements failed at 12 weeks because the collagen tissue did not have enough time to mature and handle the transferred mechanical load. However, the combination of neoligament and seeded TEL were able to handle some of the load transfer, thereby maintaining the ligament function. Also, during normal ligament healing, there is an initial decrease in mechanical properties for natural ACL replacements with autografts and allografts before the tissue is remodeled. Therefore, it is normal to have low strength-retention percentages during the early time points, which then increase with time.

In conclusion, we have determined that a biomimetic TEL for soft tissue regeneration can effectively regenerate the ACL. We found the combination of the TEL with ACL cells yielded better results than that of polymer replacements without cell seeding. It seems that this good functional outcome was achieved by tissue infiltration throughout the implant and more mature collagen remodeling during the transfer of load to the neoligament. Cell seeding, the textile structure of the replacement, and the surgical technique used for its installation appear to play major roles in influencing the healing response and long-term success of the TEL. The time for tissue infiltration and maturation to handle the transferred mechanical load may be more important than an extended time point to understand and evaluate the neoligament/TEL. But longer time points would be helpful in confirm-
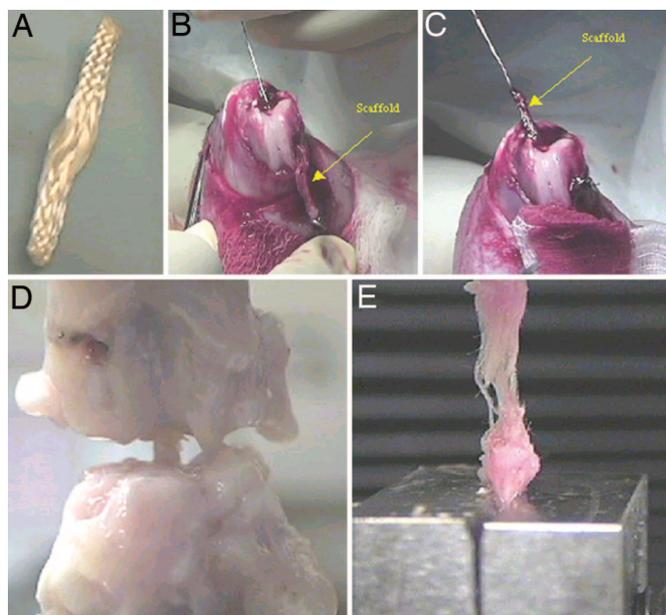
Fig. 4. TEL replacement, surgical procedure, and mechanical testing. (*A*) Fibrous hierarchy of 3D 5 × 5 square braid used as a ligament replacement. (*B* and *C*) Passage of ligament replacement through the femur bone tunnel. (*D*) Tension on ligament replacement in grips after removal of surrounding intraarticular tissue and suture buttons before mechanical testing. (*E*) Twelve-week seeded TEL tensile test to failure after mechanical pullout from the bone.

ing the results of this preliminary study that the replacement has begun to increase in strength retention. Further studies with an expanded number of samples and time points are needed to assess the long-term functionality of the TEL. The preliminary studies in this paper suggest that the potential to generate tissue-engineered ACL grafts with cells seeded onto synthetic biodegradable polymer scaffolds that can ultimately lead to a promising ligament replacement technology.

Materials and Methods

Scaffold Preparation and Characterization. Multifilament fibers of PLLA (70 denier) (Albany International Research Company, Albany, NY) were laced into 10 fibers per yarn, and 24 yarns were fabricated into a 3D square braid (Fig. 4*A*) (11). The braided scaffolds were cut to a length of 3.5–4 cm and sterilized with 70% alcohol, followed by UV irradiation. The average molecular weights (*n* = 3) for PLLA were measured by gel permeation chromatography in tetrahydrofuran by using polystyrene standards. The initial average molecular weight of the PLLA scaffolds was 196,475 ± 9,846 g/mol. The mechanical properties of the braided scaffold (*n* = 6) under tension were tested on an Instron machine, model 5544 (Instron, Canton, MA) using a 500-N load cell (gauge length = 1 cm), at a strain rate of 2% per second. The initial mechanical properties were 332 ± 20 N and 354 ± 68 MPa, respectively, at failure. The

porosity and mode pore diameter of the 3D, braided scaffolds (*n* = 6) were measured by using mercury porosimetry (AutoPore III; Micromeritics, Norcross, GA). The scaffold investigated had a porosity of 58 ± 9%, a surface area of 111 ± 8 cm^2, and a mode pore diameter of 183 ± 83 μm.

Cell Growth and ACL Reconstruction. New Zealand White rabbits received unseeded or seeded TEL (PLLA scaffold seeded with primary rabbit ACL cells). Rabbit ACL cells were isolated and cultured according to the protocols described in refs. 35 and 36. The seeded TEL replacements were seeded with 3 million ACL cells (passage 4) and incubated at 37°C with 5% CO$_2$ and at 95% humidity 2 days before implantation. At 4 and 12 weeks, the reconstructed ligaments were characterized mechanically (*n* = 6) and histologically (*n* = 3). The contralateral leg was used as a control for each animal. The replacement was fixed by interference with a suture over the button technique at the femoral and tibial tunnels (Fig. 4 *B* and *C*). Surgeries and experiments were performed according to protocols approved by the Institutional Animal Care and Use Committee of Drexel University.

Mechanical Testing. The rabbit knees to be mechanically tested were stored in PBS solution in a −20°C freezer until the start of mechanical preparation. The samples were removed 2 days before testing from the −20°C freezer and were placed in the 4°C room to allow the knees to slowly thaw (20, 21, 37). Once the legs thawed, the knee joints were dissected of all soft tissue except for the tissue around the intraarticular zone creating a femur–intraarticular zone–tibia complex (Fig. 4*D*). All intraarticular zone connective tissue was dissected, except for the ACL, just before testing. The resting gauge length of the ligament (polymer) and the cross-sectional area of the midsubstance were estimated under slight tension with digital calipers. Each knee was positioned at 180° extension, clamped, and tested on an Instron model 5544 testing machine (Fig. 4*D*). The unseeded and seeded TEL, after being pulled from both of the bone tunnels, were placed into the grips and tested to failure at a strain rate of 2% per second (Fig. 4*E*). The TEL implants failed in the intraarticular zone. Load-deformation characteristics were analyzed at a 2% per second strain rate to failure on the basis of the estimated measured gauge length.

Histological Staining. For histological samples, the rabbit knees were dissected, fixed in 10% formalin, decalcified, and embedded in paraffin. Serial sections were made at 8-microns thickness. The sections were stained with Weigert's Massons Trichrome and Safranin O stain (38). Sections were examined for collagen tissue ingrowth, inflammation, vascular structures, giant cells, macrophages, and fibroblasts.

1. Dunn MG, Tria AJ, Kato YP, Bechler JR, Ochner RS, Zawadsky JP, Silver FH (1992) *Am J Sports Med* 20:507–515.
2. Wise DL, Trantolo DJ, Altobelli DE, Yaszemski MJ, Gresser JD, Schwartz ER (1995) *Encyclopedic Handbook of Biomaterials and Bioengineering*, Part A: Materials (Dekker, New York).
3. Altman GH, Horan RL, Lu HH, Moreau J, Martin I, Richmond JC, Kaplan DL (2002) *Biomaterials* 23:4131–4141.
4. Yahia L (1997) *Ligaments and Ligamentoplasties* (Springer, New York).
5. Guidoin MF, Marois Y, Bejui J, Poddevin N, King MW, Guidoin R (2000) *Biomaterials* 21:2461–2474.
6. Laurencin CT, Ambrosio AM, Borden MD, Cooper JA, Jr (1999) *Annu Rev Biomed Eng* 1:19–46.
7. Wise DL, Trantolo DJ, Altobelli DE, Yaszemski MJ, Gresser JD, Schwartz ER (1995) *Encyclopedic Handbook of Biomaterials and Bioengineering*, Part A: Applications (Dekker, New York).
8. Wise DL, Trantolo DJ, Altobelli DE, Yaszemski MJ, Gresser JD, Schwartz ER (1995) *Encyclopedic Handbook of Biomaterials and Bioengineering*, Part B: Applications (Dekker, New York).
9. Greco RS (1994) *Implantation Biology: The Host Response and Biomedical Devices* (CRC, Boca Raton, FL).
10. Middleton JC, Tipton AJ (1998) *Med Plastic Biomaterials* 5:31–38.

11. Cooper JA, Jr (2002) *Design, Optimization and in Vivo Evaluation of a Tissue-Engineered Anterior Cruciate Ligament Replacement* (UMI Dissertation Publishing, Ann Arbor, MI).
12. Cooper JA, Jr, Bailey LO, Carter JN, Castiglioni CE, Kofron MD, Ko FK, Laurencin CT (2006) *Biomaterials* 27:2747–2754.
13. Cooper JA, Lu HH, Ko FK, Freeman JW, Laurencin CT (2005) *Biomaterials* 26:1523–1532.
14. Lu HH, Cooper JA, Jr, Manuel S, Freeman JW, Attawia MA, Ko FK, Laurencin CT (2005) *Biomaterials* 26:4805–4816.
15. Laitinen O, Tormala P, Taurio R, Skut, Saarelainen K, Iivonen T, Vainionpaa S (1992) *Biomaterials* 13:1012–1016.
16. Azangwe G, Mathias KJ, Marshall D (2001) *Clin Biomech (Bristol, Avon)* 16:913–917.
17. Black J (1992) *Biological Performance of Materials: Fundamentals of Biocompatibility* (Dekker, New York).
18. Amis AA, Kempson SA, Campbell JR, Miller JH (1988) *J Bone Joint Surg Br* 70:628–634.
19. Hart RA, Woo SL, Newton PO (1992) *J Orthop Res* 10:96–103.
20. Ballock RT, Woo SL, Lyon RM, Hollis JM, Akeson WH (1989) *J Orthop Res* 7:474–485.
21. Danto MI, Woo SL (1993) *J Orthop Res* 11:58–67.
22. Engle C, Noguchi M, Ohland KJ, Shelley FJ, Woo SL (1994) *J Orthop Res* 12:357–364.
23. Mendes E, Lopes JM, Castro C, Oliveira J (1998) *Knee* 5:9–19.
24. Jackson DW (1984) *Am J Sports Med* 12:255–257.
25. Carlstedt CA, Nordin M (1989) in *Basic Biomechanics of the Musculoskeletal System*, eds Nordin M, Frankel VH (Lea & Febiger, Philadelphia) pp 59–74.
26. Smith BA, Livesay GA, Woo SL (1993) *Clin Sports Med* 12:637–670.
27. Nordin M, Frankel VH, eds (1989) *Basic Biomechanics of the Musculoskeletal System* (Lea & Febiger, Philadelphia).
28. Noyes FR, Butler DL, Grood ES, Zernicke RF, Hefzy MS (1984) *J Bone Joint Surg Am* 66:344–352.
29. Arnoczky SP, Warren RF, Ashlock MA (1986) *J Bone Joint Surg Am* 68:376–385.
30. Nigg BM, Herzog W (1994) *Biomechanics of the Musculo-Skeletal System* (Wiley, New York).
31. Woo SL, Debski RE, Withrow JD, Janaushek MA (1999) *Am J Sports Med* 27:533–543.
32. Black J, Hastings G (1998) *Handbook of Biomaterial Properties* (Chapman & Hall, London).
33. Woo SL, Livesay GA, Engle C (1992) *Orthopaedic Review* 935–941.
34. Laitinen O, Pohjonen T, Tormala P, Saarelainen K, Vasenius J, Rokkanen P, Vainionpaa S (1993) *Arch Orthop Trauma Surg* 112:270–274.
35. Nagineni CN (1998) *J Orthop Res* 10:465–475.
36. Freshney IR (1994) *Culture of Animal Cells: A Manual of Basic Technique* (Wiley, New York).
37. Ohno K, Yasuda K, Yamamoto N, Kaneda K, Hayashi K (1996) *Clin Biomech (Bristol, Avon)* 11:207–213.
38. Prophet EB, Mills B, Arrington JB, Sobin LH (1994) *Laboratory Methods in Histotechnology* (American Registry of Pathology, Washington, DC).